Interaction Between Closely Packed Array Antenna Elements Using Meta-Surface for Applications Such as MIMO Systems and Synthetic Aperture Radars

**Mohammad Alibakhshikenari[1]** iD, **Bal S. Virdee[2]** iD, **Panchamkumar Shukla[2]**, **Chan H. See[3]** iD, **Raed Abd-Alhameed[4]** iD, **Mohsen Khalily[5]** iD, **Francisco Falcone[6]**, and **Ernesto Limiti[1]** iD

[1]Electronic Engineering Department, University of Rome "Tor Vergata", Rome, Italy, [2]Center for Communications Technology, School of Computing and Digital Media, London Metropolitan University, London, UK, [3]School of Engineering, University of Bolton, Bolton, UK, [4]School of Electrical Engineering and Computer Science, University of Bradford, Bradford, UK, [5]5G innovation Center (5GIC), Institute for Communication Systems (ICS), University of Surrey, Guildford, UK, [6]Electric and Electronic Engineering Department, Universidad Pública de Navarra, Pamplona, Spain

Abstract The paper presents a technique to enhance the isolation between adjacent radiating elements that is common in densely packed antenna arrays. Such antennas provide frequency beam-scanning capability needed in multiple-input multiple-output (MIMO) systems and synthetic aperture radars. The method proposed here uses a metamaterial decoupling slab (MTM-DS), which is located between radiating elements, to suppress mutual coupling between the elements that would otherwise degrade the antenna efficiency and performance in both the transmit and receive mode. The proposed MTM-DS consists of mirror imaged E-shaped slits engraved on a microstrip patch with inductive stub. Measured results confirm over 9–11 GHz with no MTM-DS the average isolation (S_{12}) is -27 dB; however, with MTM-DS the average isolation improves to -38 dB. With this technique the separation between the radiating element can be reduced to $0.66\lambda_0$, where λ_0 is free space wavelength at 10 GHz. In addition, with this technique there is 15% improvement in operating bandwidth. At frequencies of high impedance match of 9.95 and 10.63 GHz the gain is 4.52 and 5.40 dBi, respectively. Furthermore, the technique eliminates poor front-to-back ratio encountered in other decoupling methods. MTM-DS is also relatively simple to implement. Assuming adequate space is available between adjacent radiators the MTM-DS can be fixed retrospectively on existing antenna arrays, which makes the proposed method versatile.

1. Introduction

With the advent of 5G mobile communications multiple-input multiple-output (MIMO) systems are expected to play a major role. This is because MIMO antennas provide advantages of increased data rate, reliability, quality, and channel capacity. Moreover, MIMO system can mitigate the effects of multipath fading. However, one of the main challenges in the design of MIMO antennas is isolation reduction between adjacent closely spaced antennas with a spacing of less than a wavelength at the operating frequency. Suppressing the coupling between radiating elements in MIMO reduces degradation in the corresponding impedance and radiation properties (Al-Hasan et al., 2015; Bernety & Yakovlev, 2015; Pan et al., 2016). Mutual coupling also encountered in antenna arrays is mainly attributed to three factors, that is, (i) signal leakage via surface waves along the substrate, (ii) coupling between the feedlines through conducting current on the metallic background, and (iii) coupling due to the spatial electromagnetic (EM) fields (Pan et al., 2016). Surface waves have a significant impact on the mutual coupling when microstrip substrate thickness h is greater than $0.3\lambda_0/(2p/\sqrt{\varepsilon_r})$ (James & Henderson, 1979), where λ_0 is the operating wavelength in free space, p is a positive integer and ε_r is the relative permittivity of the dielectric substrate. Surface wave coupling diminishes only by 3 dB when the distance between the antennas is doubled. Over recent years numerous techniques have been proposed to reduce the mutual coupling between antenna radiating elements in the design of antenna arrays. In Amendola et al. (2005) and Jackson et al. (1993), shorted patches have been used to negate excitation of the surface wave modes. In Yang et al. (2005), EM band gap (EBG) structures are employed to suppress mutual coupling. Defected ground structures (DGS) have also been investigated to suppress mutual coupling (Guha et al., 2008). In fact, DGS resonators have been used in various applications including microwave filters and matching circuits as well as suppressing harmonic and
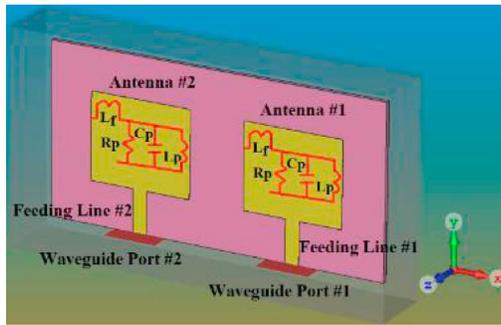
(a) Isometric view of the patch antennas. The equivalent circuit model is annotated, where L_f represents the feedline inductance, R_p the patch resistance, C_p the patch capacitance, and L_p the patch inductance.
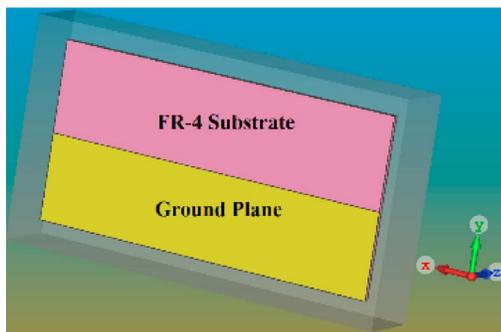
(b) back view (ground plane)

Figure 1. Configuration of 2 × 1 antenna array constructed on FR-4 lossy substrate with thickness of h = 1.6 mm, dielectric constant of ε_r = 4.3 and $tan\delta$ = 0.025. (a) Isometric view of the patch antennas. The equivalent circuit model is annotated, where L_f represents the feedline inductance, R_p the patch resistance, C_p the patch capacitance, and L_p the patch inductance. (b) back view (ground plane).

cross-polarization in microstrip antennas (Guha et al., 2006; Liu et al., 2005; Ting et al., 2006). Compared with EBG structures, the advantage of DGS is that it can be used to realize bandgap effect with a more compact circuit size. In Shafique et al. (2015) mutual coupling is suppressed by 14 dB in a densely packed antenna by using metamaterial structures etched in the ground plane and the top layer; however, the antenna's front-to-back ratio is poor. In a recent work, side-lobe suppression of 4.3 dB has been achieved using complementary split-ring resonator loading in the ground plane of antenna array (Wahid et al., 2015). Use of slot combined complementary split-ring resonator structure etched in the ground plane and on the top layer of the antenna array is shown to provide coupling suppression of 19 dB (Qamar et al., 2014). With this technique, however, the front-to-back ratio is deteriorated. A meta-surface wall isolator has been introduced in Alibakhshikenari et al. (2018) to enhance the isolation between the array antennas. By this method, a maximum mutual coupling suppression of 13.5 dB has been achieved. Other coupling suppression techniques using metamaterial or EBG suffer from either complex fabrication process or large separation between radiating elements (Farsi et al., 2012; Hafezifard et al., 2016; Qamar et al., 2016; Tang et al., 2011).

In this paper, mutual coupling between radiating elements is reduced significantly using metamaterial decoupling slab (MTM-DS) in closely packed antenna arrays that are used in MIMO and synthetic aperture radar systems. In the proposed technique, the MTM-DS is deployed between the radiating antennas. MTM-DS can be applied retrospectively subject to sufficient spacing between the radiating elements, which makes the technique versatile. With this technique the edge-to-edge separation between the radiators can be reduced to $0.66\lambda_0$, where the free space wavelength is at 10 GHz. Measured results confirm the mutual coupling between the antennas is suppressed on average by 38 dB from 9 to 11 GHz. The paper is organized as follows. In section 2, the antenna array without MTM-DS is first characterized and its simplified equivalent circuit model is presented. Next, the MTM-DS is characterized and applied in the antenna array. This structure's equivalent circuit model is compared with the full-wave EM model. Decoupling effect by the proposed MTM-DS is next confirmed using surface current plots over the antenna array. In section 3, parametric study on the MTM-DS is performed to gain an insight of how the physical parameters of the structure affect its performance. Measured and simulated results of the antenna array without and with MTM-DS are presented in section 4. The radiation patterns of the antenna array are given in section 5 along with comparison with other techniques reported to date. The work is concluded in section 6.

2. Antenna Design

2.1. Antenna Array With No MTM-DS

Structure of 2 × 1 element microstrip patch, which constitutes the unit cell of an antenna array is shown in Figure 1 where the waveguide ports are applied to the feedlines for simulation purpose. The ground plane is truncated to enhance the impedance bandwidth of the two-element antenna array. Individual patch antennas are modeled as parallel *RLC* resonant circuits whose radiation impedance is function of feedline position. The two identical patch antennas have dimensions L = 18.77 mm and W = 16.43 mm.

Input impedance of each microstrip patch antenna, shown in Figure 2, was computed using 3-D full-wave EM simulation tool, that is, CST Microwave Studio. In the simulation, all the boundary conditions were specified as "open (added space)," which assumes that no external conditions are applied to the antenna. Under this condition the simulator effectively places perfectly matched microwave absorber material at the boundary, which guarantees the antenna array is in open space. The equivalent circuit model parameters given in
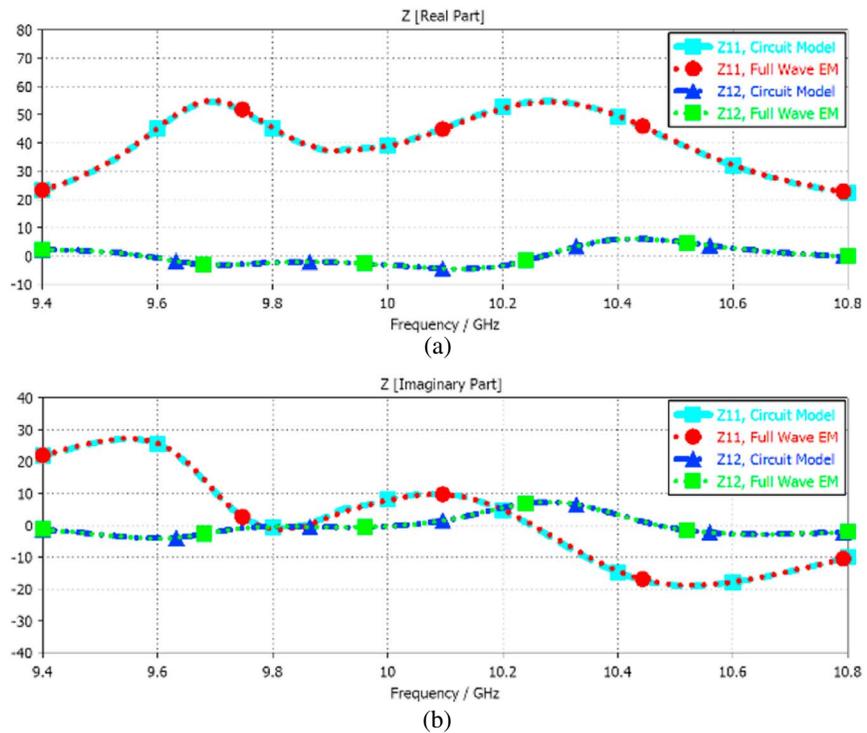
Figure 2. Input impedances (Ω) of a single antenna element.

Table 1 were extracted using optimization method in CST Microwave Studio over a specified frequency range. This is the reason why the mapping is coherent.

The simulated reflection and transmission coefficient response of the antenna array as a function of gap (d) between the antennas is shown in Figure 3. Coupling behavior between the two identical patches in Figure 1 was also analyzed. In the analysis the ground plane was represented as a perfect electric conductor boundary. Coupling coefficient was extracted from the transmission coefficient response of the structure. Frequency of the resonance peaks corresponding to the two patches, that is, f_1 and f_2, were used to determine the coupling coefficient k_{12} using the following relation (Chang & Hsieh, 2004):

$$k_{12} = \frac{f_2^2 - f_1^2}{f_2^2 + f_1^2} \tag{1}$$

Coupling coefficient is plotted in Figure 3c as a function of the gap (d) between the patches. It shows the coupling coefficient reduces linearly with increasing the gap between the patches.

The simplified equivalent circuit model of the two-element patch antenna array is shown in Figure 4. EM coupling between the two patches is represented by coupling coefficient k_{12}. Microstrip patches are represented by parallel *RLC* resonant circuit whose values are given in Table 2. As the two antennas are identical the magnitude of their characterizing parameters is the same. Figure 5 shows the circuit model response matches exactly with the full-wave EM simulation response. This figure shows that the proposed array operates over 9.56–10.63 GHz, with bandwidth of 1.07 GHz and fractional bandwidth of 10.6%. In addition, impedance matching is particularly good at two resonance frequencies of $f_{r_1} = 9.76$ GHz and $f_{r_2} = 10.24$ GHz. At these frequencies the isolation between elements is $S_{12} = -31$ and -24 dB, respectively.

Table 1
Extracted Parameters Representing the Equivalent Circuit Model of the Patch Antenna

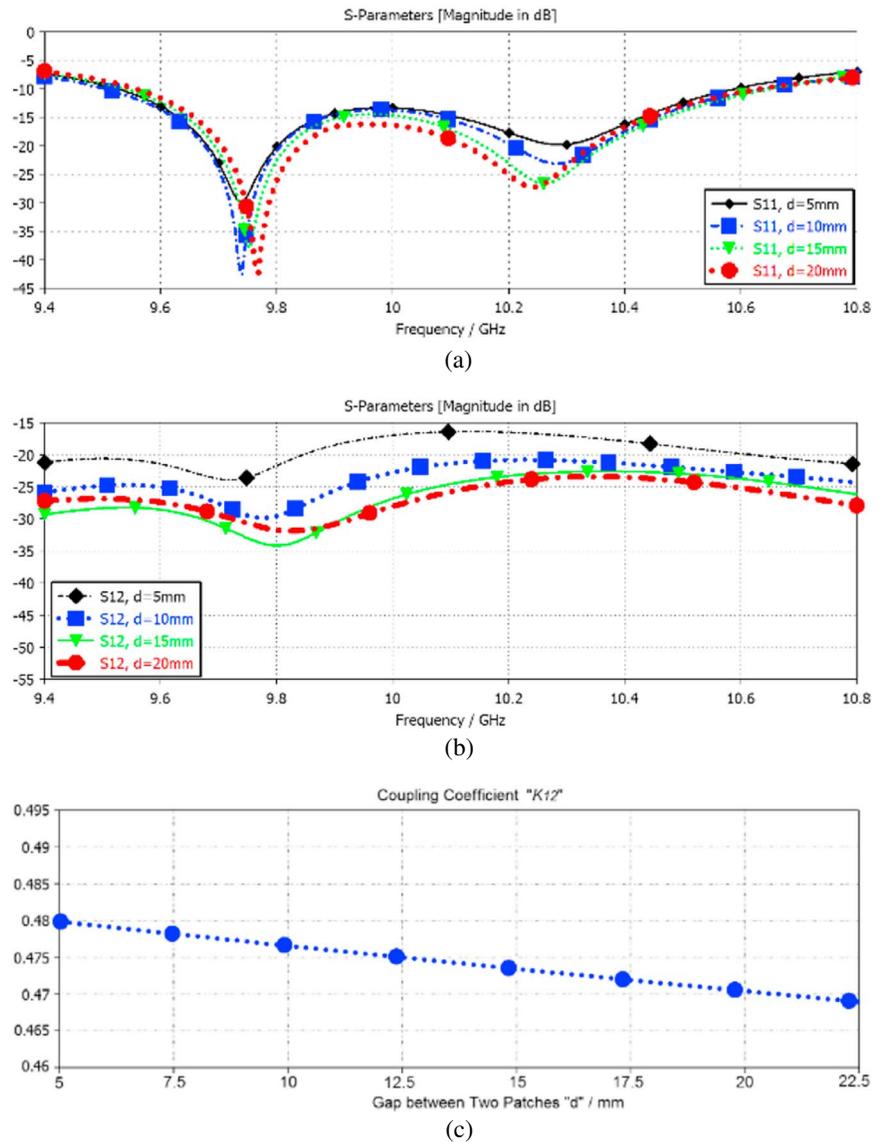| Parameter	Value
R_p	55 Ω
C_p	15.9 pF
L_p	0.2 nH
L_f	2 nH

Note. Lumped elements are annotated in Figure 1.

Figure 3. (a–b) Reflection and transmission coefficient response and (c) coupling coefficient as a function of gap between the two patches.

2.2. Metamaterial Decoupling Slab (MTM-DS)

Metamaterial property of negative permeability and permittivity exhibited by slotted patch antenna is well established and described in detail in Paul et al. (2017), Yu et al. (2017), and Pyo et al. (2009). Structure of the MTM-DS proposed here, which is shown in Figure 6, was determined from simulation
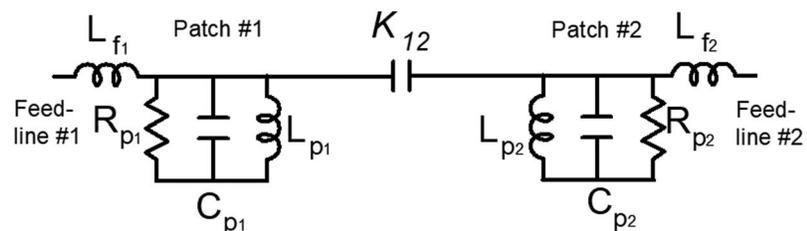

Figure 4. Equivalent circuit model of two-element basic antenna array of Figure 1.

Table 2
Equivalent Circuit Parameters of the Two-Element Antenna Array Antenna in Figure 4

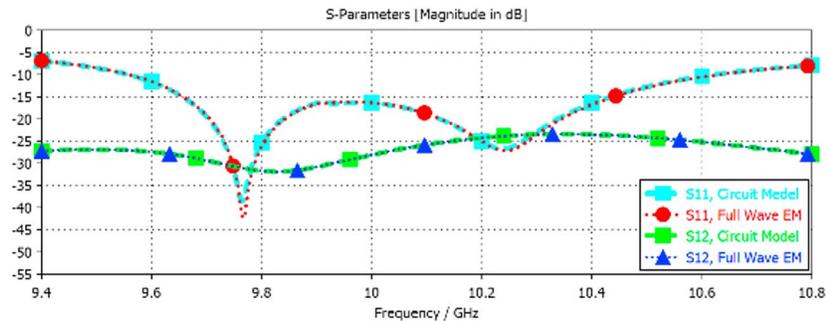| Parameter	Value
R_P	55 Ω
C_P	16.2 pF
L_P	0.2 nH
L_F	2.2 nH
K_{12}	0.047

Figure 5. Reflection and transmission coefficient response (S_{11} and S_{12}) of the proposed two-element antenna array.
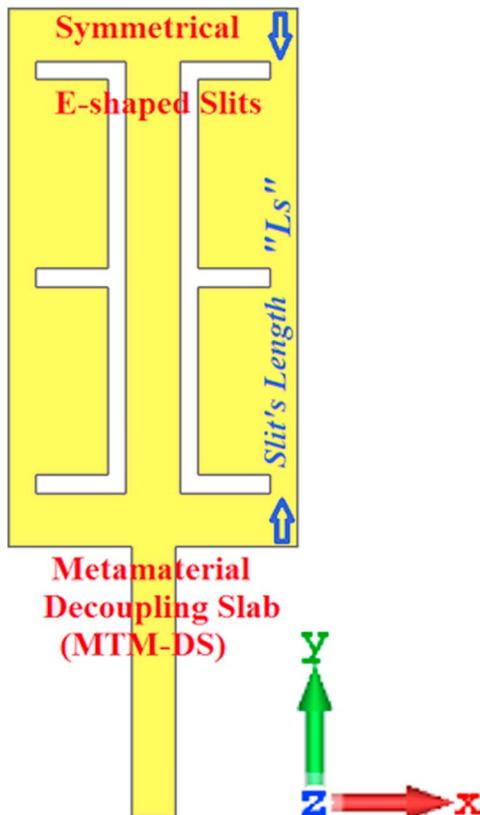

Figure 6. The structure of the proposed metamaterial decoupling slab, where surface waves propagate along the *x*-axis, H‖*y*, E‖*z*.

analysis. It consists of two E-shaped slits that are etched in a rectangular microstrip patch with a high impedance open-circuited stub at the bottom. The E-shaped slits are arranged as a mirror image. The E-shaped slits are essentially capacitive in nature, and the high impedance stub of quarter wavelength length acts like grounded inductance. The equivalent electrical circuit of the decoupling slab corresponds to that of a metamaterial structure (Caloz & Itoh, 2005). As the proposed MTM-DS configuration is free of metal via its fabrication is considerably economic. MTM-DS was fabricated on the same substrate as the patch elements, that is, FR-4 lossy substrate of 1.6-mm thickness and dielectric constant of 4.3. Optimized dimensions of the MTM-DS structure are given in Table 3.

Constitutive parameters, that is, permittivity and permeability, of MTM-DS were calculated from the scattering parameters of the structure using the technique proposed by Smith et al. (2005). Scattering parameters, permittivity and permeability of the MTM-DS structure are plotted in Figure 7 as a function of slot length (*Ls*). The resonator exhibits negative permittivity ($\varepsilon < 0$) and negative permeability ($\mu < 0$) in regions of the frequency spectrum confined between 8 to 12 GHz, which is characteristic if metamaterials. The E-shaped slits enable fine tuning of the structures resonant frequency without varying other parameters.

2.3. Planar Antenna Array with MTM-DS

MTM-DS was incorporated in the patch antenna array, as shown in Figure 8, and fabricated on the same substrate that was specified earlier. Microstrip stub attached to the MTM-DS is an open circuit. Dimensions of the radiation patches and MTM-DS are 18.77 × 16.43 mm^2 and 8.96 × 16.43 mm^2, respectively. The edge-to-edge separation between the radiating patch elements is 0.66λ$_0$, where λ$_0$ is free space wavelength at 10 GHz. Each patch is individually fed by a microstrip feedline. The dimensions of the structure in Figure 8 are given in Table 3.

Table 3
Dimensions (in mm) of 1 × 2 Antenna Array With MTM-DS

#1	#2	#3	#4	#5	#6	#7	#8
57.58	25.17	18.77	16.43	2.13	8.96	5.3	2.77
#9	#10	#11	#12	#13	#14	#15	#16
0.52	0.52	1.71	1.28	5.54	8.53	67.41	16.21

2.3.1. Equivalent Circuit Model

In Figure 8 the E-fields are polarized along *z*-axis and the coupling between the patches is along the *x*-axis. The simplified equivalent circuit model of the two-element radiating patch antenna with MTM-DS is shown in Figure 9, where the patches and MTM-DS are represented as parallel *RLC* circuit. Coupling between patch#1 and decoupling slab is
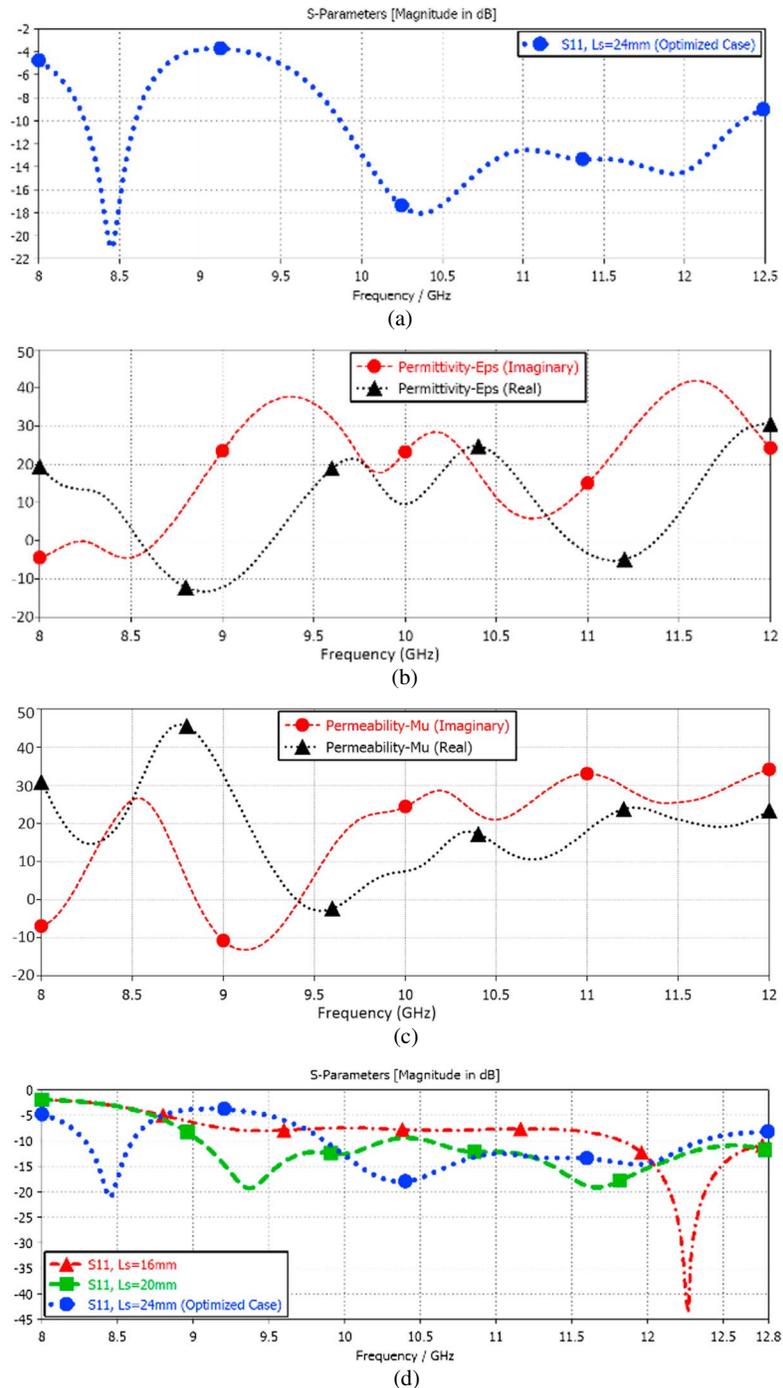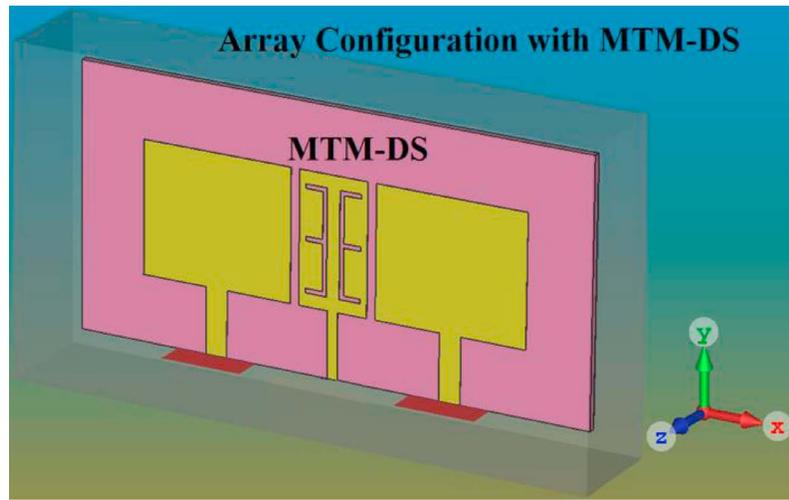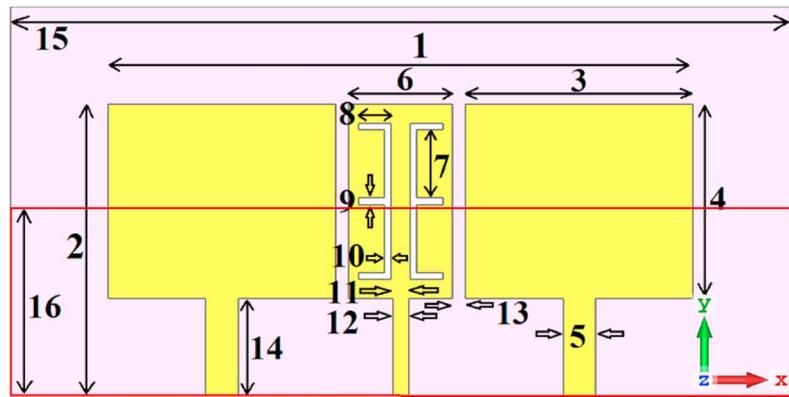

Figure 7. Metamaterial decoupling slab response: (a) S_{11}, (b) permittivity (Eps), (c) permeability (Mu), and (d) S_{11} as a function of slit length (*Ls*).

(a)

(b)

Figure 8. Geometry of 2 × 1 antenna array with MTM-DS, (a) isometric view, and (b) numerical labels define the geometry of the antenna array and MTM-DS are given in Table 3. MTM-DS = metamaterial decoupling slab.

represented by K_{DS1}; and the coupling between patch#2 and decoupling slab is represented by K_{DS2}. The extracted equivalent circuit parameters of Figure 9 are given in Table 4. Comparison of the equivalent circuit and 3-D full-wave EM simulation model responses are shown in Figure 10. S-parameters of the 2 × 1 array antenna without and with MTM-DS is shown in Figure 11.

Figure 11 reveals that when MTM-DS is inserted in the middle of the two radiating elements it introduces transmission zeros at 9.81 and 10.65 GHz, resulting in significant mutual coupling suppression of −55 and −67.50 dB, respectively. MTM-DS has effectively improved the mutual coupling suppression at the two notch frequencies by 24 and 43.57 dB, respectively. The performance of antenna array without and with MTM-DS is summarized in Table 5.
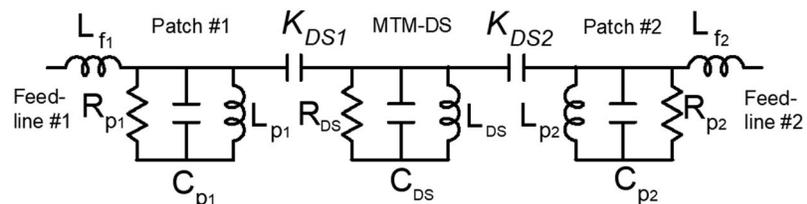

Figure 9. Simplified equivalent circuit of two-element radiating patch with MTM-DS. MTM-DS = metamaterial decoupling slab.

Table 4
Elements Values for Two-Element Array Antenna With MTM-DS

Parameter	Value
L_F	2.2 nH
R_P	55 Ω
C_P	16.2 pF
L_P	0.2 nH
K_{DS}	0.0095
R_{DS}	2200 Ω
C_{DS}	2.25 pF
L_{DS}	1.5 nH

Note. Parameters of the two radiating patches are identical including K_{DS1} and K_{DS2}.

Decoupling effects can also be observed by visualizing the surface current density plots over the 2×1 antenna array. With MTM-DS strong currents are induced on the patch antenna, as shown in Figure 12, which clearly verifies the effectiveness of the MTM-DS in suppressing surface current wave interaction between the two patches.

3. Parametric Study on MTM-DS

In this part a parametric study is presented on the proposed MTM-DS to understand the effects of the E-shaped slits on the array's performance. The following sections describe the influence of E-shaped slit width and the gap between the slits.
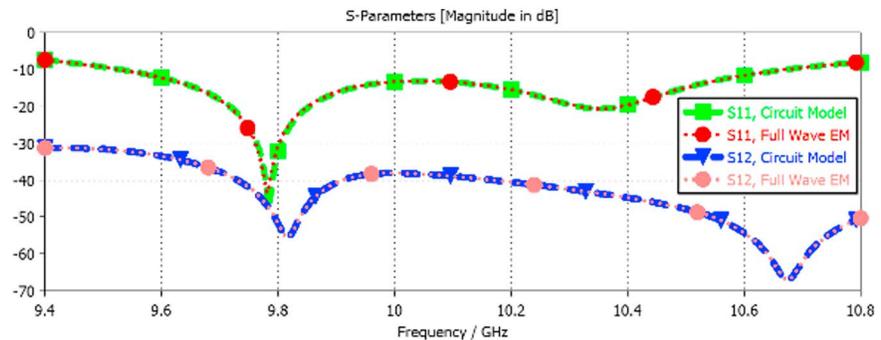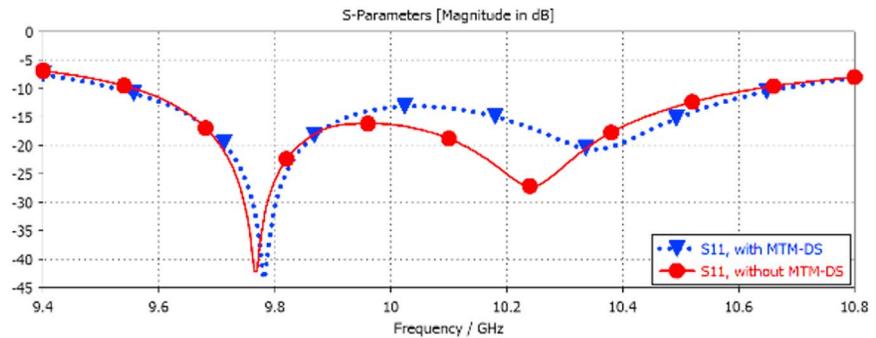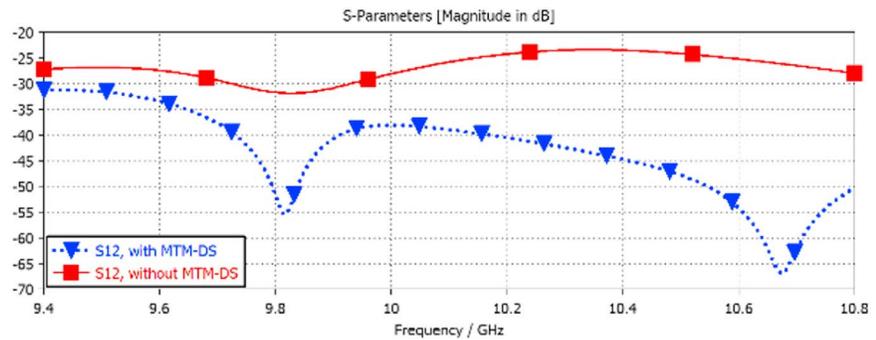

Figure 10. Comparison of S-parameter response of the circuit and EM models for the 2×1 antenna array with metamaterial decoupling slab.

(a)

(b)

Figure 11. S-parameter response of 2×1 antenna without and with MTM-DS antenna array. MTM-DS = metamaterial decoupling slab.

**Table 5**
Two-Element Antenna Array Without and With MTM-DS

| Case	Operating freq. range (GHz)	Bandwidth (GHz) for $S_{11} \leq -10$ dB	Fractional bandwidth (%)	Impedance match (dB)	
				Notch freq. #1	Notch freq. #2
Without MTM-DS	9.56–10.63	1.07	9.43	−42.17	−27.15
With MTM-DS	9.52–10.67	1.15	8.78	−43.23	−20.57
		Isolation (S_{12})			
Without MTM-DS				−30.97	−23.93
With MTM-DS				−55	−67.50

3.1. Effect of Width of Slits

The influence of width of E-shaped slits (W_1) on reflection and transmission coefficients (S_{11} and S_{12}) is shown in Figure 13. It is evident that when W_1 is increased from 0.5 to 1.25 mm the antenna's reflection coefficient or impedance match improves from −27 to −44 dB at around 9.8 GHz. In Figure 13c when W_1 is increased from 0.5 to 1.25 mm the isolation between the array's elements improves from −34 to −55 dB at around 9.8 GHz, and from −53 dB to notch −66.5 dB at around 10.65 GHz. The optimum value of W_1 is 1.25 mm.

3.2. Effect of Slit Gap

Figures 14a and 14b show the E-shape slit gap (W_2) has negligible effect on the reflection coefficient (magnitude and phase) response. Figure 14c shows the isolation significantly improves at around 9.8 and 10.6 GHz when W_2 is increased from 1 to 3 mm by 10 and 37 dB, respectively. When W_2 is increased to 4 mm the improvement diminishes due to overlapping between slot and edge of slab. The optimum gap is 3 mm.
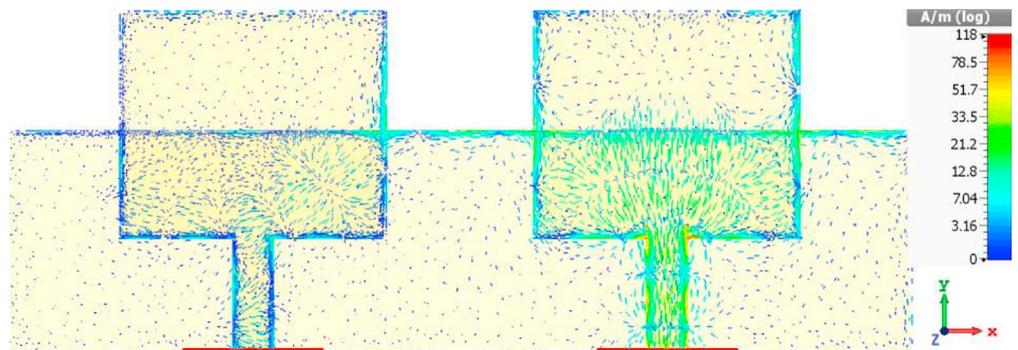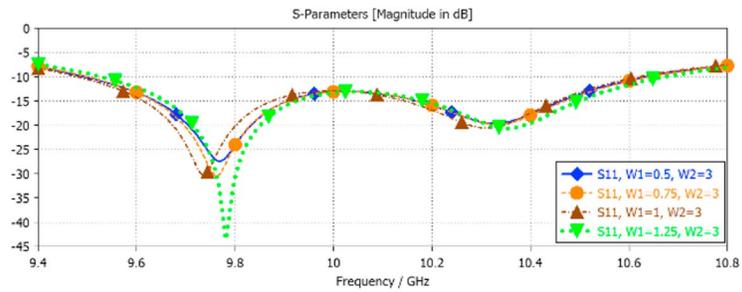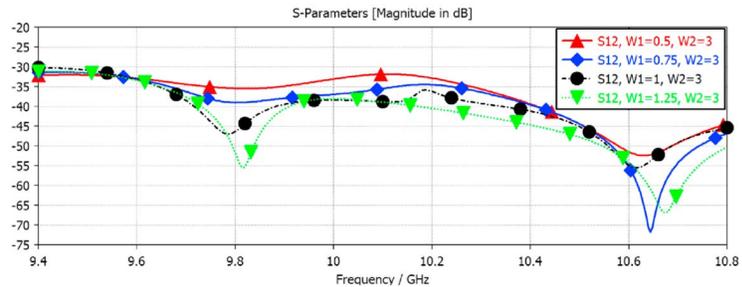

(a) without MTM-DS
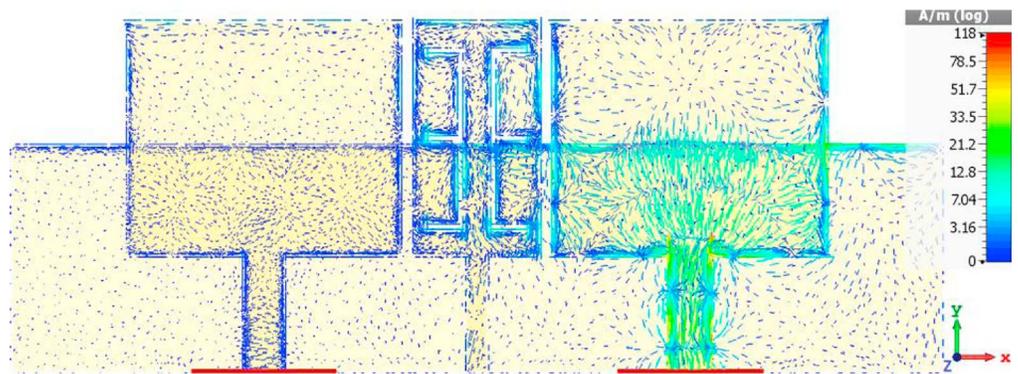
(b) with MTM-DS

Figure 12. Surface current density plots to validate the effect of MTM-DS at 10.65 GHz. MTM-DS = metamaterial decoupling slab.

(a) Reflection-coefficient

(b) Transmission-coefficient (S_{12})

Figure 13. Parametric study on slit width (W_1) when the gap between the E-shaped slits is fixed at 3 mm.

4. Measured Results

Photograph of the patch antenna array without and with MTM-DS are shown in Figure 15. The measured response of the reflection and transmission coefficients is shown in Figure 16. It shows the mutual coupling between radiating elements is reduced over a large frequency span from 9 to 11 GHz using the
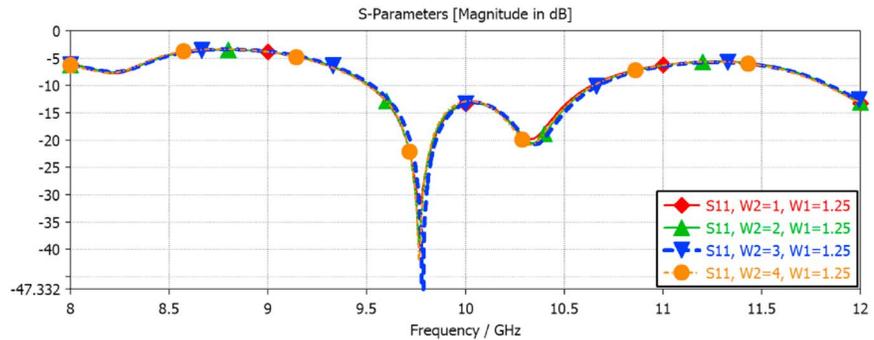
(a) Reflection-coefficient (S_{11})
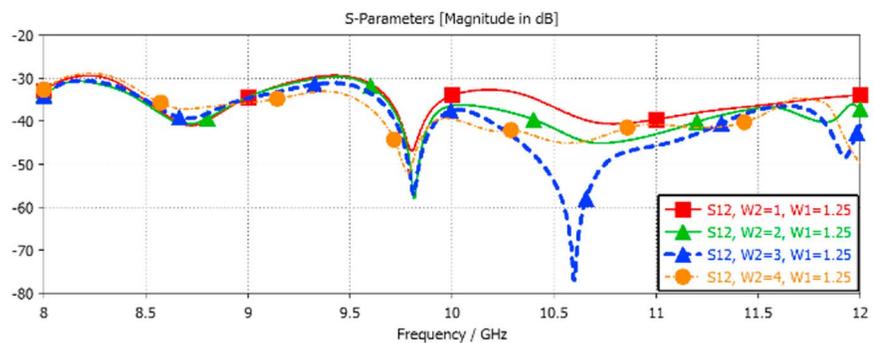
(b) Transmission coefficient (S_{12})

Figure 14. Effect of gap between the E-shaped slits (W_2) when slit width (W_1) is fixed at 1.25 mm.

(a) Top view, without MTM-DS

(b) Bottom view, without MTM-DS

(c) Top view, with MTM-DS

(d) Bottom view, with MTM-DS

Figure 15. Photographs of the antenna array with no MTM-DS and with MTM-DS. The antenna array is constructed on FR-4 lossy substrate with thickness of h = 1.6 mm, dielectric constant of ε_r = 4.3 and $tan\delta$ = 0.025. MTM-DS = metamaterial decoupling slab.

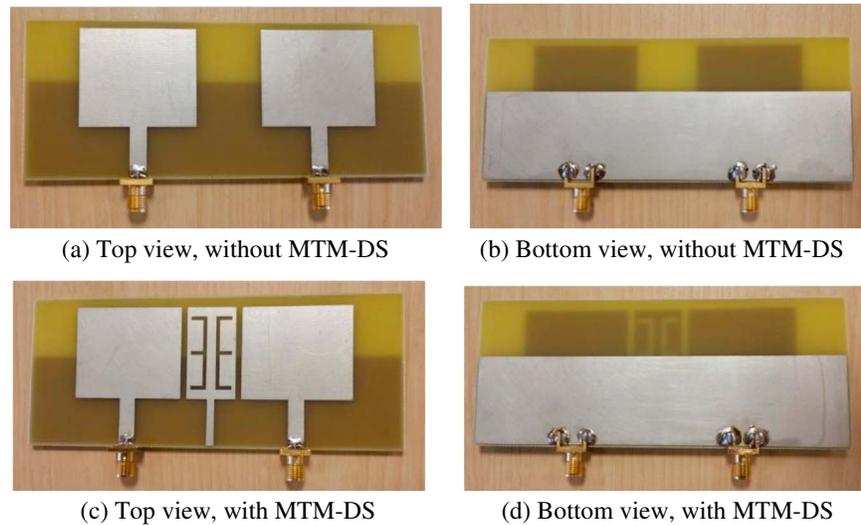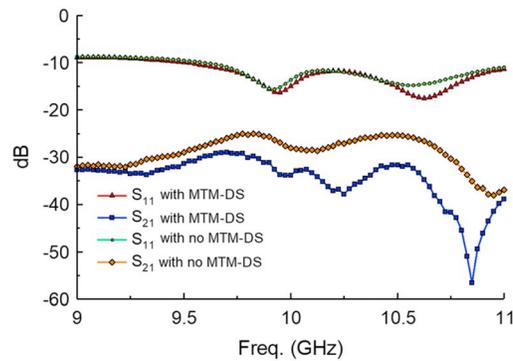**Figure 16.** Measured reflection-coefficient (S_{11}) and transmission-coefficient (S_{12}) response without and with MTM-DS. MTM-DS = metamaterial decoupling slab.

proposed MM-DS. In fact, the measured isolation with MTM-DS at 9.95 GHz is −34 dB, at 10.25 GHz is −37 dB, and at 10.85 GHz is −57 dB. However, without MTM-DS, the measured isolation at 9.95 GHz is −27 dB, at 10.25 GHz is −26 dB, and at 10.85 GHz is −37 dB. The results show improvement in isolation from 9.4 to 11 GHz. In addition, impedance matching is particularly good at f_{r_1} = 9.95 GHz and f_{r_2} = 10.63 GHz. At these frequencies, the isolation between elements is −34 and −34.8 dB, respectively. Measured S-parameter results are summarized in Table 6. Without MTM-DS the average isolation over 9 to 11 GHz is −27 dB, and with MTM-DS it is −38 dB. On average the isolation is improved by 11 dB.

Table 6
Measured Antenna Array Parameters

Bandwidth (BW) defined for S_{11} < −10 dB			
Without MTM-DS	BW = 1.3 GHz (9.6–10.9 GHz), Fractional bandwidth = 12.68%	@f_{r_1} = 9.90 GHz impedance match = −16 dB	@f_{r_2} = 10.55 GHz impedance match = −15 dB
With MTM-DS	BW = 1.6 GHz (9.4–11.0 GHz), Fractional bandwidth = 15.68%	@f_{r_1} = 9.95 GHz impedance match = −16 dB	@f_{r_2} = 10.63 GHz impedance match = −18 dB

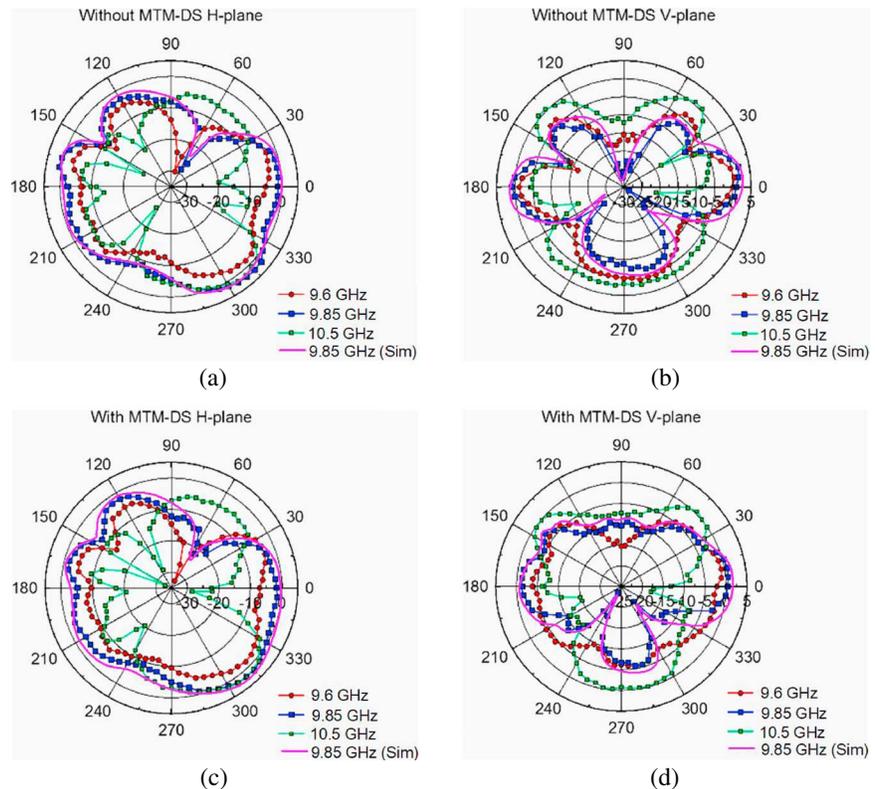| *Mutual coupling suppression between adjacent antennas (S_{12})*			
	Minimum	Average	Maximum
Without MTM-DS	−25 dB	−27 dB	−37 dB
With MTM-DS	−29 dB	−38 dB	−57 dB

Figure 17. Measured and simulated polar plots of the antenna array without and with MTM-DS at spot frequencies in horizontal and vertical planes. MTM-DS = metamaterial decoupling slab.

5. Radiation Patterns of the Proposed Array Antenna

The measured 2-D radiation plots for the antenna array without and with MTM-DS at various frequencies are shown in Figure 17. Also plotted is the simulated radiation pattern at 9.85 GHz, which shows good correlation with the measured plot at the same frequency. These plots show the effect of MTM-DS in the magnetic-plane is minimal. Although there is some effect in the electric-plane however this is not considerable. In fact, the gain is improved with MTM-DS at 9.85 GHz at an angle of 90°. A standard anechoic chamber was used to measure the antenna's gain where a transmitting horn antenna was located at the focal point of the reflector to convert the spherical waves to plane waves directed towards the antenna under test. The antenna gain was measured using the standard comparative method with the antennas fed in-phase. Connector losses were considered in the measurements.

The simulated 3-D far-field radiation patterns at frequencies of high impedance match in Figure 18 show there is good correlation without and with application of MTM-DS. These results confirm there is little impact with MTM-DS on the pattern specifications. It is also observed in Figure 18 that the radiation patterns are more directive with the proposed MTM-DS. Gain at 9.95 and 10.63 GHz are 4.31 and 4.85 dBi, respectively, without MTM-DS; and 4.52 and 5.40 dBi, respectively, after applying the MTM-DS.

Comparison of the proposed technique with other methods reported to date in Table 7. It is clear the proposed technique offers significantly higher mutual coupling suppression with closely spaced radiators and is relatively easy to construct and integrate in densely packed array antenna. It removes the drawback of poor front-to-back-ratio reported in other decoupling techniques. In addition to high-coupling suppression, the MTM-DS can be retrofitted subject to sufficient space between the antennas which makes this technique versatile for various applications having stringent performance requirements. One drawback of the proposed technique compared to (Qamar et al., 2016) is that the radiation patterns is affected over its wider operational bandwidth.
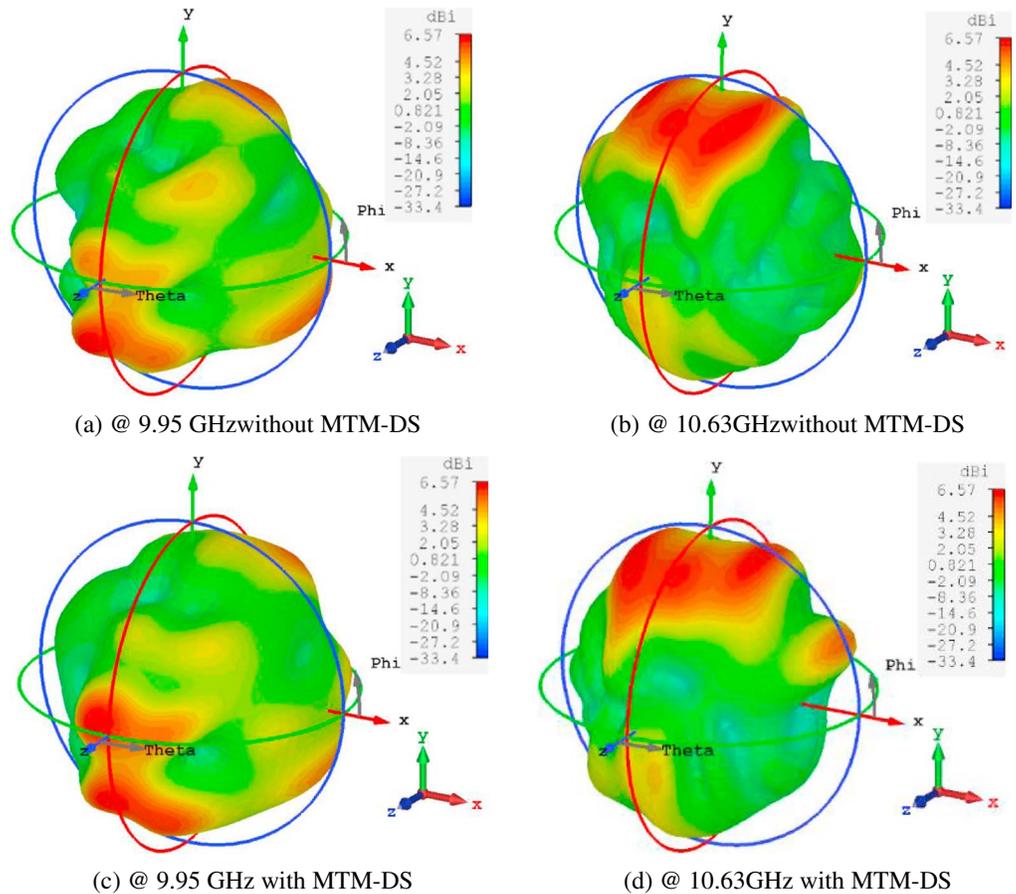
(a) @ 9.95 GHzwithout MTM-DS

(b) @ 10.63GHzwithout MTM-DS

(c) @ 9.95 GHz with MTM-DS

(d) @ 10.63GHz with MTM-DS

Figure 18. Three-dimensional radiation patterns without and with MTM-DS at high impedance matching frequencies. MTM-DS = metamaterial decoupling slab.

As advantages of the proposed work than Alibakhshikenari et al. (2018) we can mention that the maximum mutual coupling suppression here by the proposed technique is 57 dB that shows more than 43 dB improvement than Alibakhshikenari et al. (2018). As well as, the minimum and average mutual coupling suppressions presented by this work show more than 22 and 28 dB improvements compared with Alibakhshikenari et al. (2018). Here edge-by-edge distance between the radiation elements is $0.66\lambda_0$, but in Alibakhshikenari et al. (2018) this parameter is $1.16\lambda_0$. One more point, regarding the different operating frequency bands the antenna arrays have different applications than each other.

Table 7
Comparison of the Proposed Mutual Coupling Suppression Technique With Other Reported Techniques

Ref.	Mutual coupling suppression technique	Maximum mutual coupling suppression (dB)	Patch separation (λ_0)	Operating bandwidth reduction (%)	Design complexity
Amendola et al., 2005	Shorted annular elliptical patch (SAEP)	8	0.75	19	Moderate
Jackson et al., 1993	Ring of magnetic current	10	0.5	13	Moderate
Shafique et al., 2015	Complementary split-ring resonators (CSRR)	37	0.125	0	High
Wahid et al., 2015	Complementary split-ring resonators (CSRR)	10	0.25	22	High
Alibakhshikenari et al., 2018	meta-surface wall isolator	13.5	1.16	0	Low
Qamar et al., 2016	Complementary split-ring resonator (CSRR)	27	0.125	29	Low
Farsi et al., 2012	U-shaped microstrip line	17	0.75	12	Moderate
Tang et al., 2011	Periodically grounded edge-coupled split-ring resonators (PGE-SRRs)	18	0.5	0	High
This work	**MTM-DS**	**57**	**0.66**	**0**	**Low**

6. Conclusion

An effective technique is presented for suppressing mutual coupling encountered in antenna arrays. This involves inserting MTM-DS between the radiating elements. With the proposed technique the edge-to-edge separation between the antennas in the antenna array can be reduced to $0.66\lambda_0$, where the free-space wavelength is at 10 GHz. MTM-DS comprises two E-shaped slits arranged in a mirror image that are engraved on a rectangular patch. MTM-DS is shown to effectively minimize mutual coupling between adjacent radiators by suppressing surface wave propagation. With the proposed MTM-DS the mutual coupling suppression on average is -38 dB over 9 to 11 GHz.

References

Al-Hasan, M. J., Denidni, T. A., & Sebak, A. R. (2015). Millimeter-wave compact EBG structure for mutual coupling reduction applications. *IEEE Transactions on Antennas and Propagation*, *63*(2), 823–828. https://doi.org/10.1109/TAP.2014.2381229

Alibakhshikenari, M., Virdee, B. S., Shukla, P., See, C. H., Abd-Alhameed, R., Falcone, F., & Limiti, E. (2018). Meta-surface wall suppression of mutual coupling between microstrip patch antenna arrays for THz-band applications. *Progress In Electromagnetics Research Letters*, *75*, 105–111. https://doi.org/10.2528/PIERL18021908

Amendola, G., Boccia, L., & Massa, G. (2005). Shorted elliptical patch antennas with reduced surface waves on two frequency bands. *IEEE Transactions on Antennas and Propagation*, *53*(6), 1946–1956. https://doi.org/10.1109/TAP.2005.848469

Bernety, H. M., & Yakovlev, A. B. (2015). Reduction of mutual coupling between neighboring strip dipole antennas using confocal elliptical metasurface cloaks. *IEEE Transactions on Antennas and Propagation*, *63*(4), 1554–1563. https://doi.org/10.1109/TAP.2015.2398121

Caloz, C., & Itoh, T. (2005). *Electromagnetic metamaterials: Transmission line theory and microwave applications*. Wiley. https://doi.org/10.1002/0471754323

Chang, K., & Hsieh, L.-H. (2004). *Microwave ring circuits and related structure*. Wiley.

Farsi, S., Aliakbarian, H., Schreurs, D., Nauwelaers, B., & Vandenbosch, G. A. (2012). Mutual coupling reduction between planar antennas by using a simple microstrip U-section. *IEEE Antennas and Wireless Propagation Letters*, *11*, 1501–1503.

Guha, D., Biswas, S., Biswas, M., Siddiqui, J. Y., & Antar, Y. M. M. (2006). Concentric ring-shaped defected ground structures for microstrip applications. *IEEE Antennas and Wireless Propagation Letters*, *5*(1), 402–405. https://doi.org/10.1109/LAWP.2006.880691

Guha, D., Biswas, S., Joseph, T., & Sebastian, M. T. (2008). Defected ground structure to reduce mutual coupling between cylindrical dielectric resonator antennas. *Electronics Letters*, *44*(14), 836–837. https://doi.org/10.1049/el:20081189

Hafezifard, R., Naser-Moghadasi, M., Mohassel, J. R., & Sadeghzadeh, R. A. (2016). Mutual coupling reduction for two closely spaced meander line antennas using metamaterial substrate. *IEEE Antennas and Wireless Propagation Letters*, *15*, 40–43.

Jackson, D. R., Williams, J. T., Bhattacharyya, A. K., Smith, R. L., Buchheit, S. J., & Long, S. A. (1993). Microstrip patch designs that do not excite surface waves. *IEEE Transactions on Antennas and Propagation*, *41*(8), 1026–1037. https://doi.org/10.1109/8.244643

James, J. R., & Henderson, A. (1979). High-frequency behavior of microstrip open-circuit terminations. *IEE Journal on Microwaves, Optics and Acoustics*, *3*(5), 205–218. https://doi.org/10.1049/ij-moa.1979.0046

Liu, H., Li, Z., Sun, X., & Mao, J. (2005). Harmonic suppression with photonic bandgap and defected ground structure for a microstrip patch antenna. *IEEE Microwave and Wireless Components Letters*, *15*(2), 55–56.

Pan, B. C., Tang, W. X., Qi, M. Q., Ma, H. F., Tao, Z., & Cui, T. J. (2016). Reduction of the spatially mutual coupling between dual-polarized patch antennas using coupled metamaterial slabs. *Nature Scientific Reports*, *6*, 1–8.

Paul, L. C., Haque, M. A., Haque, M. A., Rashid, M. M. U., Islam, M. F., & Rahman, M. M. (2017). Design a slotted metamaterial microstrip patch antenna by creating three dual isosceles triangular slots on the patch and bandwidth enhancement, 3rd International Conference on Electrical Information and Communication Technology (EICT), 7-9 Dec. 2017, Khulna, Bangladesh.

Pyo, S., Baik, J.-W., Cho, S.-H., & Kim, Y.-S. (2009). Metamaterial-based antenna with triangular slotted ground for efficiency improvement. *Electronics Letters*, *45*(3), 144–146. https://doi.org/10.1049/el:20092424

Qamar, Z., Naeem, U., Khan, S. A., Chongcheawchamnan, M., & Shafique, M. F. (2016). Mutual coupling reduction for high-performance densely packed patch antenna arrays on finite substrate. *IEEE Transactions on Antennas and Propagation*, *64*(5), 1653–1660. https://doi.org/10.1109/TAP.2016.2535540

Qamar, Z., Riaz, L., Chongcheawchamnan, M., Khan, S. A., & Shafique, M. F. (2014). Slot combined complementary split ring resonators for mutual coupling suppression in microstrip phased arrays. *IET Microwaves, Antennas and Propagation*, *8*(15), 1261–1267. https://doi.org/10.1049/iet-map.2013.0541

Shafique, M. F., Qamar, Z., Riaz, L., Saleem, R., & Khan, S. A. (2015). Coupling suppression in densely packed microstrip array using metamaterial structure. *Microwave and Optical Technology Letters*, *57*(3), 759–763. https://doi.org/10.1002/mop.28943

Smith, D. R., Vier, D. C., Koschny, T., & Soukoulis, C. M. (2005). Electromagnetic parameter retrieval from inhomogeneous metamaterials. *Physical Review E*, *71*(3), 036617. https://doi.org/10.1103/PhysRevE.71.036617

Tang, M. C., Xiao, S., Wang, B., Guan, J., & Deng, T. (2011). Improved performance of a microstrip phased array using broadband and ultra-low loss metamaterial slabs. *IEEE Antennas and Propagation Magazine*, *53*(6), 31–41. https://doi.org/10.1109/MAP.2011.6157712

Ting, S.-W., Tam, K.-W., & Martins, R. P. (2006). Miniaturized microstrip lowpass filter with wide stopband using double equilateral U-shaped defected ground structure. *IEEE Microwave and Wireless Components Letters*, *16*(5), 240–242. https://doi.org/10.1109/LMWC.2006.873592

Wahid, A., Sreenivasan, M., & Rao, P. H. (2015). CSRR loaded microstrip array antenna with low side lobe level. *IEEE Antennas and Wireless Propagation Letters*, *14*, 1169–1171.

Yang, L., Fan, M. Y., Chen, F. L., She, J. Z., & Feng, Z. H. (2005). A novel compact electromagnetic bandgap structure and its applications for microwave circuits. *IEEE Transactions on Microwave Theory and Techniques*, *53*(1), 183–190. https://doi.org/10.1109/TMTT.2004.839322

Yu, B., Li, Q., Wang, H., Li, Y., & Yang, G. (2017). Metamaterial-based low-profile broadband hexagonal-grid-slotted patch antenna, International Applied Computational Electromagnetics Society Symposium (ACES), 1-4 Aug. 2017, Suzhou, China.